Desalination and Water Treatment
www.deswater.com
doi: 10.1080/19443994.2014.880158

54 (2015) 562–571
April

Taylor & Francis
Taylor & Francis Group

Kinetics and isotherm of cationic dye removal from multicomponent system using the synthesized silica nanoparticle

Niyaz Mohammad Mahmoodi*, Adonis Maghsoodi

Department of Environmental Research, Institute for Color Science and Technology, Tehran, Iran
Tel. +98 021 22969771; Fax: +98 021 22947537; emails: mahmoodi@icrc.ac.ir; nm_mahmoodi@aut.ac.ir

Received 17 July 2013; Accepted 22 December 2013

ABSTRACT

In this paper, silica nanoparticle was synthesized. Dye removal ability of the synthesized silica nanoparticle (SSN) from single and multicomponent (ternary) systems was studied. The SSN was characterized by fourier transform infrared and scanning electron microscopy. Basic Red 18 (BR18), Basic Red 46 (BR46) and Basic Violet 16 (BV16) were used as cationic dyes. The kinetics and isotherm of dye adsorption were studied. The effect of operational parameter such as adsorbent dosage and initial dye concentration was evaluated. Adsorption kinetic of dyes was found to conform to pseudo-second-order kinetics. The maximum dye adsorption capacity (Q_0) of SSN for BR18, BR46 and BV16 were 98, 88 and 416 mg/g, respectively. It was found that adsorption of BR18, BR46 and BV16 onto SSN followed with Freundlich isotherm. The results showed that the SSN being an eco-friendly adsorbent might be a suitable alternative to remove cationic dyes from multicomponent systems.

Keywords: Silica nanoparticles; Synthesis; Dye removal; Ternary system; Kinetics and isotherm

1. Introduction

The spread of pollutants in aqueous media has become a critical issue worldwide because of rapid development of industrialization, population growth, etc. Different methods such as adsorption, photocatalysis, ozonation and oxidation were used to treat wastewater. Coloured wastewater is as a consequence of dyeing process because high amount of the total world production of dyes is lost during dyeing [1–9].

Adsorption of pollutants using adsorbent materials is widely used to treat wastewater [10]. Most of the adsorbents are easily available and low-cost but they have some disadvantages such as poor mechanical and heat resistance and relatively limited adsorption capacity for dyes [11]. Among a great variety of adsorbents, silica is of particular interest because of its stability, possible reuse and relative rapidity in reaching equilibrium, high mechanical resistance and high surface area [12]. Silica is capable to interact with various organic compounds [13,14].

Several inorganic materials were used to remove cationic dyes from single systems (Table 1) [15–21]. They have different dye adsorption capacities. In this paper, silica nanoparticle was synthesized. The synthesized silica nanoparticle (SSN) was used to remove cationic dyes from single and ternary systems (Fig. 1).

*Corresponding author.

Table 1
Cationic dye removal ability of different inorganic adsorbents

Adsorbent	Cationic dye	Q_0 (mg/g)	Ref.
Magnetic multiwall carbon nanotube nanocomposite	Methylene blue	12	[15]
	Brilliant cresyl blue	6	
Multiwalled carbon nanotube filled with Fe_2O_3	Methylene blue	42	[16]
Magnetic alginate bead	Methylene blue	9	[17]
γ-Fe_2O_3	Acridine orange	59	[18]
SBA-15	Methylene blue	51	[19]
	Janus green B	71	
Zeolite	Maxilon Goldgelb GL EC	15	[20]
	Maxilon Schwarz FBL-01	56	
Clay (Turkey)	Basic blue 9	6	[21]
SSN	Basic Red 18	98	This study
	Basic Red 46	88	
	Basic violet 16	416	

Fourier transform infrared (FTIR) and scanning electron microscopy (SEM) were used to characterize the SSN. Three cationic dyes (Basic Red 18 (BR18), Basic Red 46 (BR46) and Basic Violet 16 (BV16)) were used as model compounds. The kinetics and isotherm of dye adsorption were studied in detail. The effect of operational parameter such as adsorbent dosage and initial dye concentration was evaluated.

2. Materials and methods

2.1. Chemicals

Cationic dyes, Basic Red 18 (BR18), Basic Red 46 (BR46) and Basic Violet 16 (BV16) were obtained from Ciba and used without further purification. The chemical structure of dyes is shown in Fig. 2. All other chemicals were of analytical grade and purchased from Merck.

2.2. Synthesis of SSN

SSN (<90 nm) was synthesized in our laboratory. A 0.2 mol of tetraethyl orthosilicate was pored into a mixture of water and nonionic surfactant and mixed for 4 h at 25°C. The precipitate was filtered, washed with deionized water and dried.

2.3. Characterization of SSN

FTIR spectrum (Perkin–Elmer Spectrophotometer Spectrum One) of the SSN in the range 4,000–450 cm^{-1}

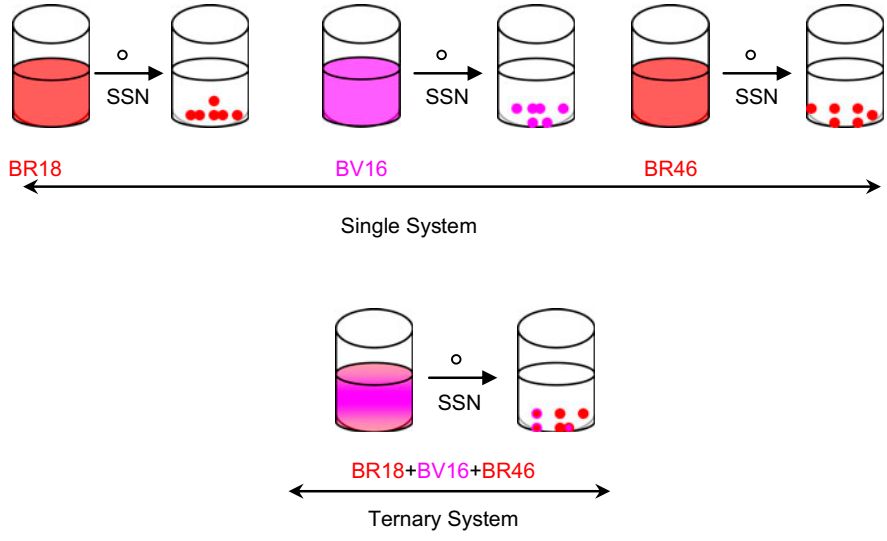

Fig. 1. Dye removal using SSN from single and ternary systems.

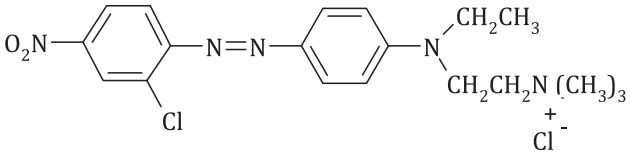

BR18

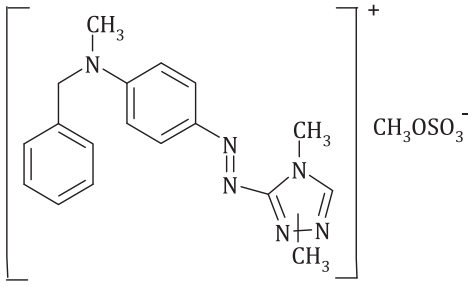

BR46

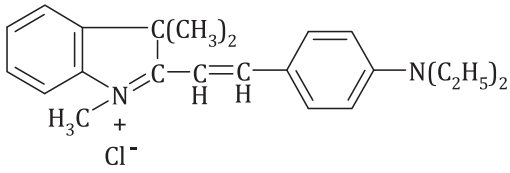

BV16

Fig. 2. The chemical structure of cationic dyes.

was studied. The morphological structure of the SSN was examined by SEM using LEO 1455VP scanning microscope.

2.4. Adsorption procedure

The dye adsorption measurements were conducted by mixing of adsorbent and dye in jars containing 250 mL of a dye solution (50 mg/L). The change on the absorbance of all solution samples were monitored and determined at certain time intervals during the adsorption process. At the end of the adsorption experiments, the solution samples were centrifuged and the dye concentration was determined. The results were verified with the adsorption isotherms and kinetics.

UV–vis spectrophotometer (Perkin–Elmer Lambda 25 spectrophotometer) was employed for absorbance measurements of samples. The maximum wavelengths (λ_{max}) used for the determination of residual concentration of BR18, BR46 and BV16 in supernatant solution using spectrophotometer were 488 nm, 532 nm and 545 nm, respectively.

The effect of adsorbent dosage on dye removal from single and ternary systems was investigated by contacting 250 mL of dye solution with initial dye concentration of 50 mg/L at room temperature (25 ˚C) for 60 min at a constant stirring speed of 200 rpm.

The effect of initial dye concentration on dye removal from single and ternary systems was investigated by contacting 250 mL of dye solution with SSN using jar test at room temperature (25 ˚C) for 60 min at a constant stirring speed of 200 rpm.

Dye concentrations were calculated as follows: for a ternary system of components A, B and C that were measured at wavelengths of λ_1, λ_2 and λ_3, respectively, to give optical densities of d_1, d_2 and d_3:

$$d_1 = k_{A1}C_A + k_{B1}C_B + k_{C1}C_C \quad (1)$$

$$d_2 = k_{A2}C_A + k_{B2}C_B + k_{C2}C_C \quad (2)$$

$$d_3 = k_{A3}C_A + k_{B3}C_B + k_{C3}C_C \quad (3)$$

$$C_A = (d_1X + d_2Y + d_3Z)/(k_{A1}X + k_{A2}Y + k_{A3}Z) \quad (4)$$

$$(X = k_{B3}k_{C2} - k_{B2}k_{C3};\ Y = k_{B1}k_{C3} - k_{B3}k_{C1};\ Z = k_{B2}k_{C1} - k_{B1}k_{C2})$$

$$C_B = (d_1X' + d_2Y' + d_3Z')/(k_{B1}X' + k_{B2}Y' + k_{B3}Z') \quad (5)$$

$$(X' = k_{A2}k_{C3} - k_{A3}k_{C2};\ Y' = k_{A3}k_{C1} - k_{A1}k_{C3};\ Z' = k_{A1}k_{C2} - k_{A2}k_{C1})$$

$$C_C = (d_1X'' + d_2Y'' + d_3Z'')/(k_{B1}X'' + k_{B2}Y'' + k_{B3}Z'') \quad (6)$$

$$(X'' = k_{A2}k_{B3} - k_{A3}k_{B2};\quad Y'' = k_{A3}k_{B1} - k_{A1}k_{B3};\ Z'' = k_{A1}k_{B2} - k_{A2}k_{B1})$$

where k_{A1}, k_{B1}, k_{C1}, k_{A2}, k_{B2}, k_{C2}, k_{A3}, k_{B3} and k_{C3} are the calibration constants for components A, B and C at the three wavelengths λ_1, λ_2 and λ_3, respectively.

3. Results and discussion

3.1. Characterization of SSN

The FTIR spectrum of the SSN is shown in Fig. 3(a). The peaks at 3,435, 1,084, 957, 801 and 470 cm^{-1} are assigned to stretching vibration of hydrogen-bonded silanol group υ(≡Si–OH), υ(–OH) of physisorbed water, υ(≡Si–O–Si≡) of siloxane backbone, υ(≡Si–OH) of free silanol group, tetrahedron ring

$\upsilon(SiO_4)$ and $\upsilon(\equiv Si–O–Si\equiv)$ deformation, respectively [22–27].

Surface morphology of the adsorbent is investigated by SEM. In addition, SEM is useful to determine the particle shape and appropriate size distribution of the adsorbent. Fig. 3(b) shows scanning electron micrograph of SSN. From Fig. 3(b), it is clear that, SSN has nanometer size.

3.2. Adsorption kinetic

The mechanism of adsorption is investigated by kinetics studies. The characteristic constants of adsorption kinetics were determined using intraparticle diffusion [28–30], pseudo-first-order equation [31] and pseudo-second-order equation [32].

The possibility of intraparticle diffusion resistance affecting adsorption was explored using the intraparticle diffusion model as [28–30]:

$$q_t = k_p t^{1/2} + I \tag{7}$$

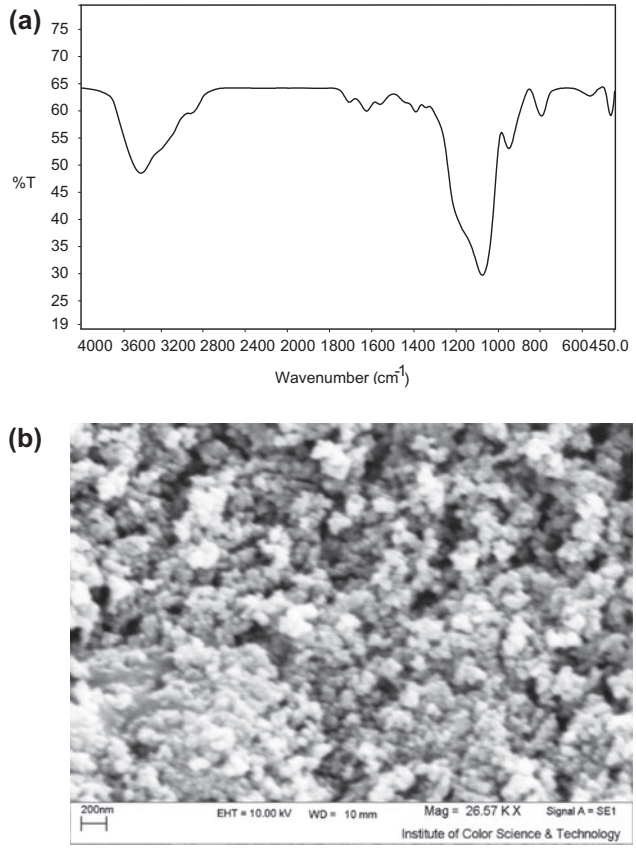

Fig. 3. Characterization of SSN (a) FTIR spectrum and (b) SEM image.

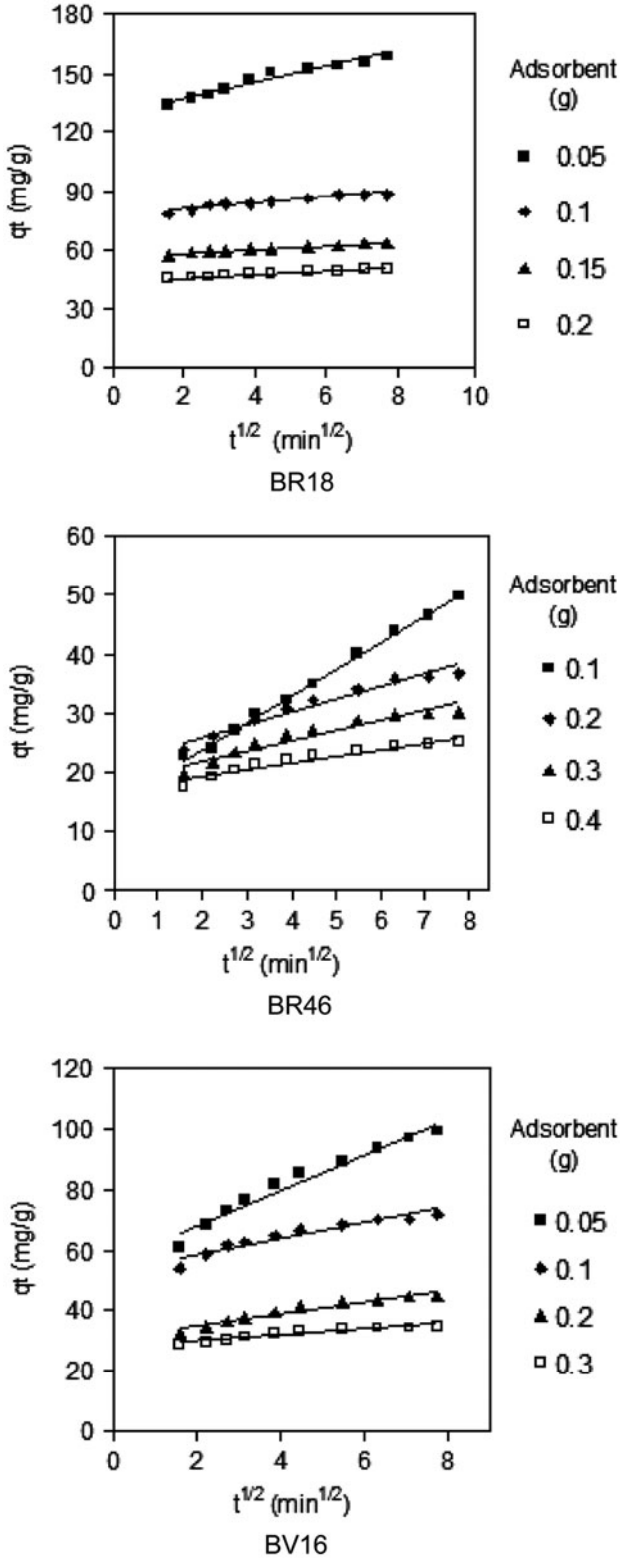

Fig. 4. Intraparticle diffusion kinetics of dye removal by SSN.

Table 2
Linearized kinetic coefficient for dye adsorption onto SSN at different adsorbent dosages ($(q_e)_{Exp}$: mg/g, $(q_e)_{Cal.}$: mg/g, k_1: 1/min, k_2: g/mg min and k_p: mg/g $min^{1/2}$)

			Intraparticle diffusion			Pseudo-first-order			Pseudo-second-order		
Dye	Adsorbent (g)	$(q_e)_{Exp.}$	k_p	I	R^2	$(q_e)_{Cal.}$	k_1	R^2	$(q_e)_{Cal.}$	k_2	R^2
BR46	0.100	50	4.504	15	0.996	32	0.044	0.986	51	0.003	0.999
	0.200	37	2.129	22	0.962	16	0.064	0.993	38	0.012	0.997
	0.300	30	1.663	19	0.922	13	0.076	0.984	31	0.017	0.998
	0.400	25	1.147	17	0.921	8	0.059	0.979	25	0.025	0.998
BV16	0.050	99	5.845	56	0.964	41	0.054	0.977	100	0.004	0.996
	0.100	72	2.645	53	0.918	16	0.048	0.974	73	0.011	0.999
	0.200	45	1.960	31	0.938	15	0.072	0.988	45	0.015	0.999
	0.300	35	0.993	28	0.939	7	0.054	0.988	35	0.030	0.999
BR18	0.050	159	3.970	129	0.953	25	0.044	0.970	158	0.007	0.999
	0.100	89	1.576	77	0.938	12	0.070	0.969	89	0.020	0.999
	0.150	63	0.889	57	0.969	6	0.053	0.977	63	0.033	0.999
	0.200	50	0.727	45	0.935	5	0.045	0.955	50	0.043	0.999

where q_t, k_p and I are the amount of dye adsorbed at time t (mg/g), the intraparticle diffusion rate constant and intercept, respectively.

To understand the applicability of the intraparticle diffusion for the dye adsorption onto SSN at different adsorbent dosages, linear plots of q_t against $t^{1/2}$ (Fig. 4), is plotted. The values of k_p, I and R^2 (correlation coefficient values) are shown in Table 2.

A linear form of pseudo-first-order model is [29,31]:

$$\log(q_e - q_t) = \log(q_e) - (k_1/2.303)t \quad (8)$$

where q_e and k_1 are the amount of dye adsorbed at equilibrium (mg/g), and the equilibrium rate constant of pseudo-first-order kinetics (1/min), respectively.

To understand the applicability of the pseudo-first-order for the dye adsorption onto SSN at different adsorbent dosages, linear plots of $\log(q_e - q_t)$ vs. contact time (t) (Fig. 5) are plotted. The values of k_1, R^2 (correlation coefficient values) and the calculated $q_e((q_e)_{Cal.})$ are shown in Table 2.

Linear form of pseudo-second-order model, was illustrated as [32]:

$$t/q_t = 1/k_2 q_e^2 + (1/q_e)t \quad (9)$$

where k_2 is the equilibrium rate constant of pseudo-second order (g/mg min).

To understand the applicability of pseudo-second order for the dye adsorption onto SSN at different adsorbent dosages, linear plots of t/q_t vs. contact time (t) (Fig. 6) are plotted. The values of k_2, R^2 (correlation coefficient values) and the calculated $q_e((q_e)_{Cal.})$ are shown in Table 2.

The linearity of the plots (R^2) demonstrates that intraparticle diffusion and pseudo-first-order kinetic models do not play a significant role in the uptake of the dye by SSN (Table 2). The linear fit between the t/q_t vs. contact time (t) and the calculated R^2 values for pseudo-second-order kinetics model shows that the dye removal kinetic can be approximated as pseudo-second-order kinetics (Table 2). In addition, the experimental $q_e((q_e)_{Exp.})$ values agree with the calculated ones ($(q_e)_{Cal.}$), obtained from the linear plots of pseudo-second-order kinetics (Table 2).

3.3. Adsorption isotherm

The adsorption isotherm expresses the relation between the mass of the dye adsorbed at a particular temperature, the pH, particle size and liquid phase of the dye concentration. Several isotherms such as Langmuir, Freundlich and Tempkin models were studied in detail.

The Langmuir isotherm which has been successfully applied to different adsorption processes can be used to explain the adsorption of dye into adsorbent. A basic assumption of the Langmuir theory is that adsorption takes place at specific sites within the adsorbent [33–35]. The Langmuir equation can be written as follows:

$$C_e/q_e = 1/K_L Q_0 + C_e/Q_0 \quad (10)$$

where C_e, K_L and Q_0 are the equilibrium concentration of dye solution (mg/L), Langmuir constant (L/g)

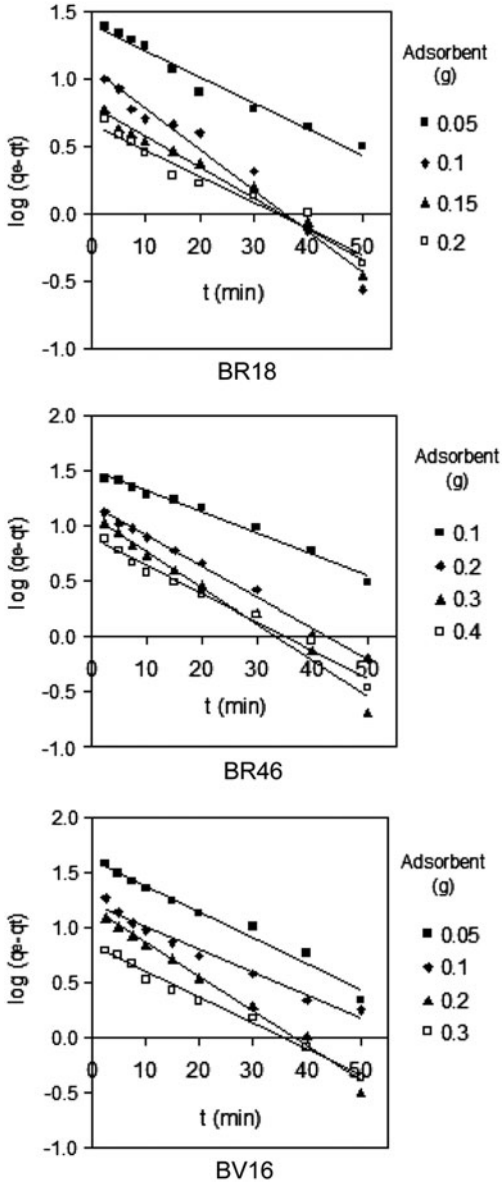

Fig. 5. Pseudo-first-order kinetics of dye removal by SSN.

and the maximum adsorption capacity (mg/g), respectively.

Also, isotherm data were tested with Freundlich isotherm that can be expressed by [36]:

$$\log q_e = \log K_F + (1/n) \log C_e \quad (11)$$

where K_F is adsorption capacity at unit concentration and $1/n$ is adsorption intensity.

$1/n$ values indicate the type of isotherm to be irreversible ($1/n = 0$), favourable ($0 < 1/n < 1$) and unfavourable ($1/n > 1$).

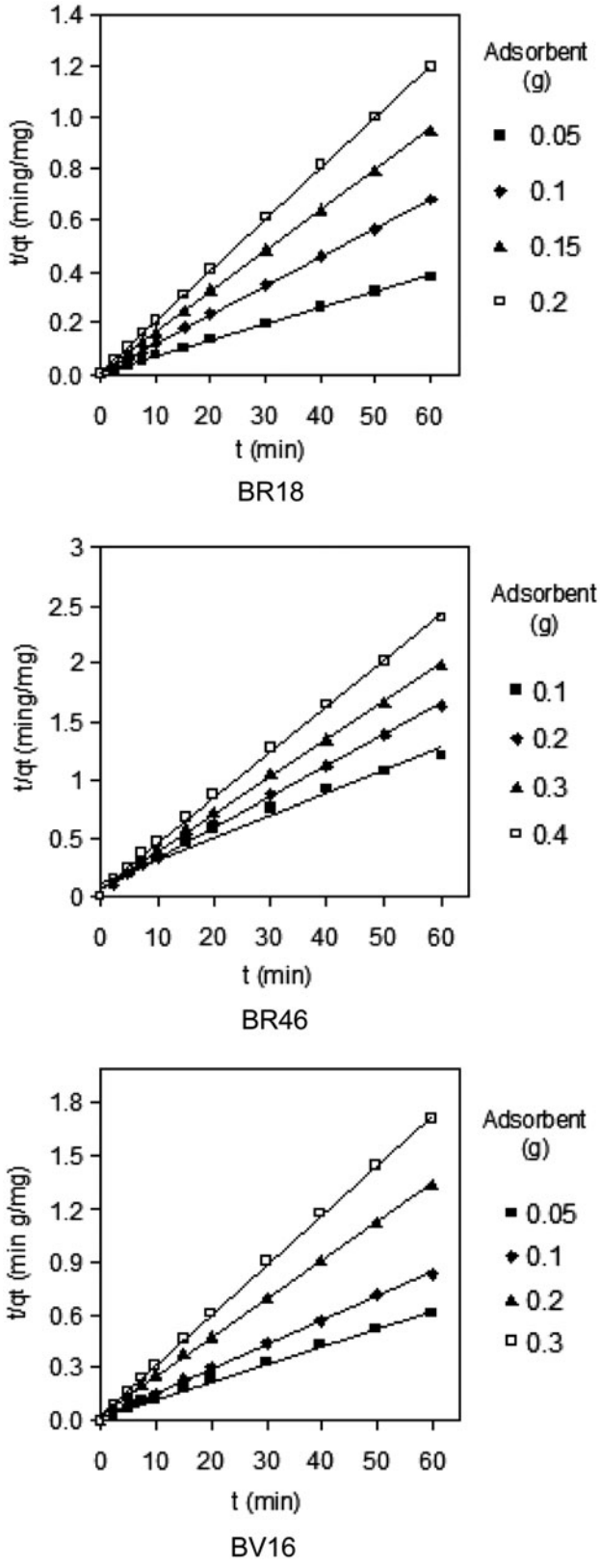

Fig. 6. Pseudo-second-order kinetics of dye removal by SSN.

Table 3
Linearized isotherm coefficients for dye adsorption onto SSN at different adsorbent dosages

	Langmuir			Freundlich			Tempkin		
Dye	Q_0	K_L	R^2	K_F	$1/n$	R^2	K_T	B_1	R^2
BR18	98	0.033	0.953	0.621	1.8824	0.970	0.125	175	0.8985
BR46	88	0.040	0.929	6.957	0.568	0.976	0.340	20	0.955
BV16	416	0.010	0.387	5.844	0.8174	0.963	0.217	49	0.917

The Tempkin isotherm is given as:

$$q_e = B_1 \ln K_T + B_1 \ln C_e \tag{12}$$

where

$$B_1 = RT/b \tag{13}$$

where K_T is the equilibrium binding constant (L/mol) corresponding to the maximum binding energy and constant B_1 is related to the heat of adsorption. In addition, R and T are the gas constant (8.314 J/mol K) and the absolute temperature (K), respectively.

Tempkin isotherm assumes that (1) the heat of adsorption of all the molecules in the layer decreases linearly with coverage due to adsorbent–adsorbate

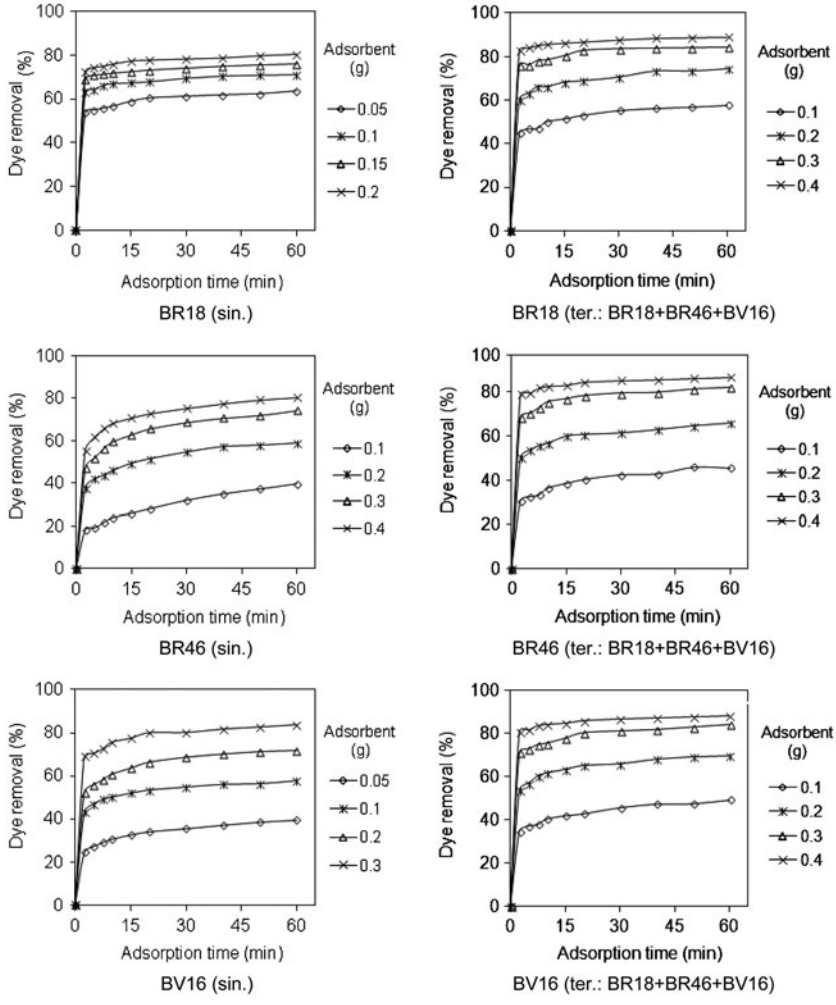

Fig. 7. The effect of adsorbent dosage on dye removal by SSN from single and ternary systems.

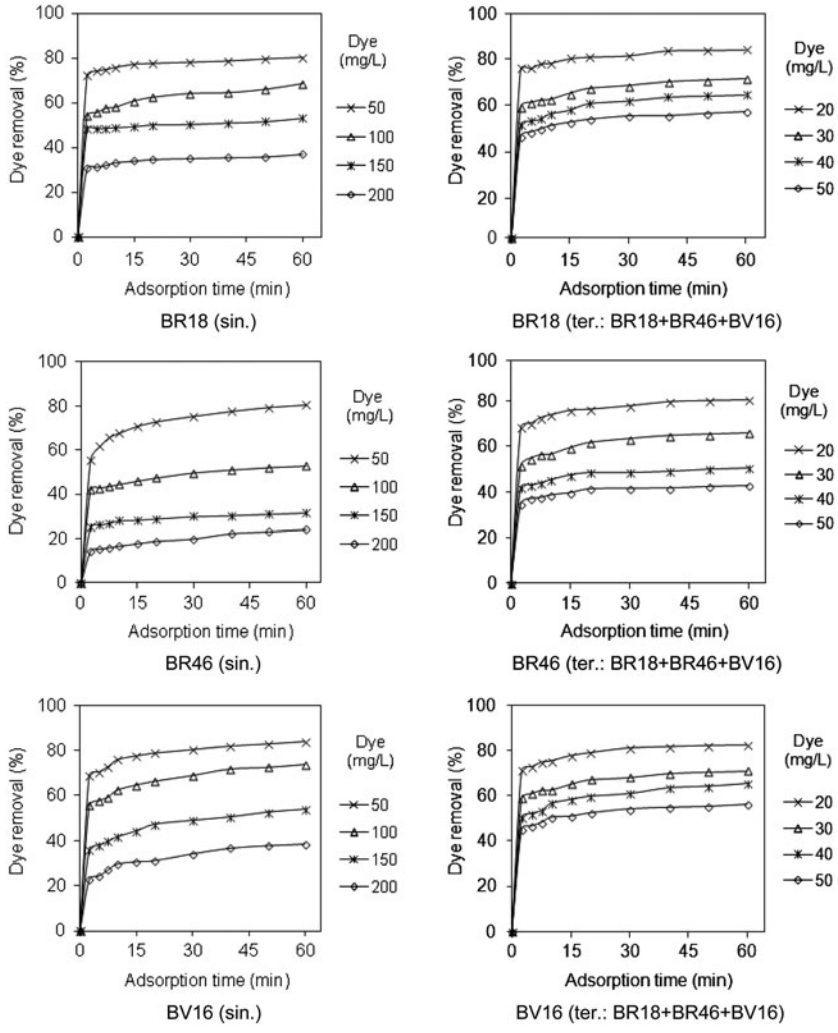

Fig. 8. The effect of dye concentration on dye removal by SSN from single and ternary systems.

interactions, and that (2) the adsorption is characterized by a uniform distribution of binding energies, up to some maximum binding energy [37,38].

To study the applicability of the Langmuir, Freundlich and Tempkin isotherms for the dye adsorption onto SSN at different adsorbent dosages, linear plots of C_e/q_e against C_e, log q_e vs. log C_e and q_e vs. ln C_e are plotted. The values of Q_0, K_L, K_F, $1/n$, K_T, B_1 and R^2 (correlation coefficient values of isotherm model) are shown in Table 3.

The correlation coefficient values (R^2) show that the dye removal isotherm using SSN does not follow the Langmuir and Tempkin isotherms (Table 3). The linear fit between the log q_e vs. log C_e and the calculated R^2 values shows that the dye removal isotherm can be approximated as the Freundlich model (Table 3). This means that the adsorption of dyes takes place at specific heterogeneous sites onto SSN surface.

The maximum adsorption capacity of several adsorbents was shown in Table 1 [15–21]. The results show that SSN has high dye adsorption capability. The maximum dye adsorption capacity (Q_0) of SSN for BR18, BR46 and BV16 were 98, 88 and 416 mg/g, respectively. Thus SSN can be used as an adsorbent to remove dyes.

3.4. Effect of operational parameter on dye removal

3.4.1. Effect of adsorbent dosage

The dye removal (%) vs. time (min) at different SSN dosages (g) from single and ternary systems was shown in Fig. 7. Dye removal increases when SSN

dosage increases (dye removal of 0.05, 0.10, 0.15 and 0.20 g SSN was 63, 70, 75 and 80% for BR18, dye removal of 0.10, 0.20, 0.30 and 0.40 g SSN was 40, 59, 74 and 80% for BR46 and dye removal of 0.05, 0.10, 0.20 and 0.30 g SSN was 40, 58, 72 and 84% for BV16). The increase in dye adsorption with adsorbent dosage can be attributed to increased adsorbent surface and availability of more adsorption sites. However, if the adsorption capacity was expressed in mg adsorbed per gram of material, the capacity decreased with the increasing amount of SSN. It can be attributed to overlapping or aggregation of adsorption sites resulting in a decrease in total adsorbent surface area available to the dye and an increase in diffusion pathlength [39].

3.4.2. Effect of dye concentration

The effect of initial dye concentration on dye removal by SSN from single and ternary systems was evaluated (Fig. 8). Dye removal of SSN at 50, 100, 150 and 200 mg/L dye concentration was 80, 68, 53 and 37% for BR18, 80, 53, 31 and 24% for BR46 and 84, 74, 54 and 38% for BV16, respectively. It is obvious that the higher the initial dye concentration, the lower the percentage of dye adsorbed. The amount of the dye adsorbed onto SSN increases with an increase in the initial dye concentration of solution if the amount of adsorbent is kept unchanged due to the increase in the driving force of the concentration gradient with the higher initial dye concentration. The adsorption of dye by SSN is very intense and reaches equilibrium very quickly at low initial concentration. At a fixed SSN dosage, the amount of dye adsorbed increased with increasing concentration of solution, but the percentage of adsorption decreased. In other words, the residual dye concentration will be higher for higher initial dye concentrations. In the case of lower concentrations, the ratio of initial number of dye moles to the available adsorption sites is low and subsequently the fractional adsorption becomes independent of initial concentration [40–44].

4. Conclusion

In this paper, the SSN was used to remove cationic dyes from single and ternary systems. Three cationic dyes, Basic Red 18 (BR18), Basic Red 46 (BR46) and Basic Violet 16 (BV16), were used as model compounds. Adsorption kinetic of dyes was found to conform to pseudo-second-order kinetics. The maximum dye adsorption capacities (Q_0) of SSN for BR18, BR46 and BV16 were 98, 88 and 416 mg/g, respectively. It was found that adsorption of BR18, BR46 and BV16 onto SSN followed with Freundlich isotherm. The results showed that the SSN being an eco-friendly adsorbent with high cationic dye adsorption capacity might be a suitable alternative to remove dyes from multicomponent systems.

References

[1] N.M. Mahmoodi, Photocatalytic ozonation of dyes using multiwalled carbon nanotube, J. Mol. Catal. A. Chem. 366 (2013) 254–260.
[2] N.M. Mahmoodi, Zinc ferrite nanoparticle as a magnetic catalyst: Synthesis and dye degradation, Mater. Res. Bullet. 48 (2013) 4255–4260.
[3] N.M. Mahmoodi, Photodegradation of dyes using multiwalled carbon nanotube and ferrous ion, J. Environ. Eng. 139 (2013) 1368–1374.
[4] N.K. Amin, Removal of reactive dye from aqueous solutions by adsorption onto activated carbons prepared from sugarcane bagasse pith, Desalination 223 (2008) 152–161.
[5] P. Xu, G.M. Zeng, D.L. Huang, C.L. Feng, S. Hu, M.H. Zhao, C. Lai, Z. Wei, C. Huang, G.X. Xie, Z.F. Liu, Use of iron oxide nanomaterials in wastewater treatment: A review, Sci. Total Environ. 424 (2012) 1–10.
[6] I.K. Konstantinou, T.A. Albanis, TiO_2-assisted photocatalytic degradation of azo dyes in aqueous solution: Kinetic and mechanistic investigations, Appl. Catal. B 49 (2004) 1–14.
[7] I. Arslan-Alaton, A review of the effects of dye-assisting chemicals on advanced oxidation of reactive dyes in wastewater, Color. Technol. 119 (2003) 345–353.
[8] Z. Aksu, Application of biosorption for the removal of organic pollutants: A review, Process Biochem. 40 (2005) 997–1026.
[9] B.K. Nandi, A. Goswami, M.K. Purkait, Adsorption characteristics of brilliant green dye on kaolin, J. Hazard. Mater. 161 (2009) 387–395.
[10] M. Özacar, İ.A. Şengil, Adsorption of reactive dyes on calcined alunite from aqueous solutions, J. Hazard. Mater. 98 (2003) 211–224.
[11] H. Yang, Q. Feng, Direct synthesis of pore-expanded amino-functionalized mesoporous silicas with dimethyldecylamine and the effect of expander dosage on their characterization and decolorization of sulphonated azo dyes, Micropor. Mesopor. Mater. 135 (2010) 124–130.
[12] A.R. Cestari, E.F.S. Vieira, G.S. Vieira, L.E. Almeida, The removal of anionic dyes from aqueous solutions in the presence of anionic surfactant using aminopropylsilica—A kinetic study, J. Hazard. Mater. 138 (2006) 133–141.
[13] M.A. Hassanien, K.S. Abouelsherbini, Synthesis and characterisation of morin-functionalised silica gel for the enrichment of some precious metal ions, Talanta 68 (2006) 1550–1559.
[14] M. Sliwkakaszynska, K. Jaszczolt, A. Kolodziejczyk, J. Rachon, 1,3-alternate 25,27-dibenzoiloxy-26,28-bis-[3-propyloxy]-calix[4]arene-bonded silica gel as a new type of HPLC stationary phase, Talanta 68 (2006) 1560–1566.
[15] S. Thurm, S. Odenbach, Magnetic separation of ferrofluids, J. Magn. Magn. Mater. 252 (2002) 247–249.

[16] J.L. Gong, B. Wang, G.M. Zeng, C.P. Yang, C.G. Niu, Q.Y. Niu, W.J. Zhou, Y. Liang, Removal of cationic dyes from aqueous solution using magnetic multi-wall carbon nanotube nanocomposite as adsorbent, J. Hazard. Mater. 164 (2009) 1517–1522.
[17] J. Sun, R. Xu, Y. Zhang, M. Ma, N. Gu, Magnetic nanoparticles separation based on nanostructures, J. Magn. Magn. Mater. 312 (2007) 354–358.
[18] V. Rocher, J.M. Siaugue, V. Cabuil, A. Bee, Removal of organic dyes by magnetic alginate beads, Water Res. 42 (2008) 1290–1298.
[19] C.H. Huang, K.P. Chang, H.D. Ou, Y.C. Chiang, C.F. Wang, Adsorption of cationic dyes onto mesoporous silica, Micropor. Mesopor. Mater. 141 (2011) 102–109.
[20] V. Meshko, L. Markovska, M. Mincheva, A.E. Rodrigues, Adsorption of basic dyes on granular activated carbon and natural zeolite, Water Res. 35 (2001) 3357–3366.
[21] A. Gürses, S. Karaca, Ç. Doğar, R. Bayrak, M. Açıkyıldız, M. Yalçın, Determination of adsorptive properties of clay/water system: Methylene blue sorption, J. Colloid Interface Sci. 269 (2004) 310–314.
[22] H. Yang, Q. Feng, Direct synthesis of pore-expanded amino-functionalized mesoporous silicas with dimethyldecylamine and the effect of expander dosage on their characterization and decolorization of sulphonated azo dyes, Micropor. Mesopor. Mater. 135 (2010) 124–130.
[23] H. Yang, Q. Feng, Characterization of pore-expanded amino-functionalized mesoporous silicas directly synthesized with dimethyldecylamine and its application for decolorization of sulphonated azo dyes, J. Hazard. Mater. 180 (2010) 106–114.
[24] A.M. Donia, A.A. Atia, W.A. Al-amrani, A.M. El-Nahas, Effect of structural properties of acid dyes on their adsorption behaviour from aqueous solutions by amine modified silica, J. Hazard. Mater. 161 (2009) 1544–1550.
[25] D.D. Asouhidou, K.S. Triantafyllidis, N.K. Lazaridis, K.A. Matis, Adsorption of Remazol Red 3BS from aqueous solutions using APTES- and cyclodextrin-modified HMS-type mesoporous silicas, Colloids Surf. A 346 (2009) 83–90.
[26] J.A.A. Sales, C. Airoldi, Epoxide silylant agent ethylenediamine reaction product anchored on silica gel—Thermodynamics of cation–nitrogen interaction at solid/liquid interface, J. Non-Cryst. Solids 330 (2003) 142–149.
[27] J. Lin, J.A. Siddiqui, R.M. Ottenbrite, Surface modification of inorganic oxide particles with silane coupling agent and organic dyes, Polym. Adv. Technol. 12 (2001) 285–292.
[28] A. Özcan, A.S. Özcan, Adsorption of Acid Red 57 from aqueous solutions onto surfactant-modified sepiolite, J. Hazard. Mater. 125 (2005) 252–259.
[29] S. Senthilkumaar, P. Kalaamani, K. Porkodi, P.R. Varadarajan, C.V. Subburaam, Adsorption of dissolved reactive red dye from aqueous phase onto activated carbon prepared from agricultural waste, Bioresour. Technol. 97 (2006) 1618–1625.
[30] W.J. Weber, J.C. Morris, Kinetics of adsorption on carbon from solution, J. Sanitary Eng. Div. Am. Soc. Civ. Eng. 89 (1963) 31–60.
[31] M.A. Ashraf, M. Hussain, K. Mahmood, A. Wajid, M. Yusof, Y. Alias, I. Yusoff, Removal of acid yellow-17 dye from aqueous solution using eco-friendly biosorbent, Desalin. Water Treat. 51 (2013) 4530–4545.
[32] Y.S. Ho, Adsorption of heavy metals from waste streams by peat, PhD thesis, The University of Birmingham, Birmingham, 1995.
[33] I. Langmuir, The constitution and fundamental properties of solids and liquids. Part I. solids, J. Am. Chem. Soc. 38 (1916) 2221–2295.
[34] I. Langmuir, The constitution and fundamental properties of solids and liquids. II. Liquids 1, J. Am. Chem. Soc. 39 (1917) 1848–1906.
[35] I. Langmuir, The adsorption of gases on plane surfaces of glass, mica and platinum, J. Am. Chem. Soc. 40 (1918) 1361–1403.
[36] A. Gil, Y. El Mouzdahir, A. Elmchaouri, M.A. Vicente, S.A. Korili, Equilibrium and thermodynamic investigation of methylene blue adsorption on thermal- and acid-activated clay minerals, Desalin. Water Treat. 51 (2013) 2881–2888.
[37] M.J. Tempkin, V. Pyzhev, Recent modification to Langmiur isotherms, Acta Physiochim. USSR 12 (1940) 217–222.
[38] Y.C. Kim, C. Kim, I. Choi, S. Rengaraj, Arsenic removal using mesoporous alumina prepared via a templating method, Environ. Sci. Technol. 38 (2004) 924–931.
[39] G. Crini, F. Gimbert, C. Robert, B. Martel, O. Adam, N. Morin-Crini, The removal of Basic Blue 3 from aqueous solutions by chitosan-based adsorbent: Batch studies, J. Hazard. Mater. 153 (2008) 96–106.
[40] G. Crini, P.M. Badot, Application of chitosan, a natural aminopolysaccharide, for dye removal from aqueous solutions by adsorption processes using batch studies: A review of recent literature, Progress Polym. Sci. 33 (2008) 399–447.
[41] P.K. Dutta, K.D. Bhavani, N. Sharma, Adsorption for dyehouse effluent by low cost adsorbent (chitosan), Asian Text. J. 10 (2001) 57–63.
[42] M.S. Chiou, H.Y. Li, Adsorption behavior of reactive dye in aqueous solution on chemical cross-linked chitosan beads, Chemosphere 50 (2003) 1095–1105.
[43] S. Chatterjee, S. Chatterjee, B.P. Chatterjee, A.R. Das, A.K. Guha, Adsorption of a model anionic dye, eosin Y, from aqueous solution by chitosan hydrobeads, J. Colloid Interface Sci. 288 (2005) 30–35.
[44] N.M. Mahmoodi, Synthesis of amine-functionalized magnetic ferrite nanoparticle and its dye removal ability, J. Environ. Eng. 139 (2013) 1382–1390.